Available at
www.ComputerScienceWeb.com
POWERED BY SCIENCE DIRECT

Signal Processing 83 (2003) 2523–2538

SIGNAL PROCESSING

www.elsevier.com/locate/sigpro

Improved Wigner–Ville distribution performance by signal decomposition and modified group delay

S.V. Narasimhan[a,*,1], Malini.B. Nayak[b]

[a] *Aerospace Electronics & Systems Division, National Aerospace Laboratories, Bangalore - 560017, India*
[b] *Department of Electronics & Communication Engineering, Karnataka Regional Engineering College, National Institute of Technology Karnataka (NITK), Surathkal - 574157, India*

Received 4 October 2000; received in revised form 5 November 2002

Abstract

A new approach has been proposed for improving the performance of the Wigner–Ville distribution. This approach is based on signal decomposition and modified magnitude group delay function. Signal decomposition achieved by perfect reconstruction filter bank reduces significantly the *existence of crossterms*. The Gibbs ripple effect is due to truncation of the Wigner–Ville distribution kernel. The modified magnitude group delay function overcomes this effect without *applying any window*. Compared to those of Pseudo Wigner–Ville distribution and its versions, the proposed method has significantly improved performance in both time and frequency resolution as there is no time and frequency smoothing. Further, this method obeys better the desirable properties of time–frequency representation and has a better noise immunity.
© 2003 Elsevier B.V. All rights reserved.

Keywords: Time–frequency distribution; Wigner–Ville distribution; Gibbs ripple reduction; Group delay; Modified group delay; Perfect reconstruction filter banks; Spectral estimation

1. Introduction

The short-time Fourier transform was introduced for processing nonstationary signals. But this necessitates a tradeoff between time localization and frequency resolution. The Wigner–Ville distribution (WVD) [5] alleviates this tradeoff. The WVD at any instant is the Fourier transform (FT) of the *instantaneous autocorrelation* (IACR) sequence of *infinite lag length*. Theoretically the WVD has an infinite resolution in time due to the absence of averaging over a finite time interval. Also for infinite lag length, it has infinite frequency resolution. Practically, it is the Pseudo WVD (PWVD) that is computed which considers IACR only for a finite number of lags. In the PWVD the IACR is weighted by a *common window function* to overcome the abrupt truncation effect namely the ripples along the frequency axis, commonly known as Gibbs effect. For a given lag length, the windowing deteriorates the frequency resolution. The IACR is also referred to as WVD kernel. *The frequency resolution is referred to the main-lobe width of the FT of a window for a given length and the rectangular window has the best frequency resolution.*

* Corresponding author. Tel.: +80-527-3351; fax: +80-527-0670.
E-mail address: svn@css.cmmacs.ernet.in (S.V. Narasimhan).
[1] Presently, at Infineon Technologies, 10th floor, Discoverer Building, International Tech park, White Field Road, Bangalore-560 066, India.

0165-1684/$ - see front matter © 2003 Elsevier B.V. All rights reserved.
doi:10.1016/j.sigpro.2003.07.011

The WVD being quadratic in nature introduces crossterms, for a multi-component signal. The crossterms make the interpretation of the WVD difficult. As the crossterms oscillate along the time axis, they can be reduced by time smoothing. But this method of crossterm suppression is only *at the cost of time resolution.*

In the last two decades, the research has been aimed at effective suppression of crossterms and improvement of the frequency resolution, preserving the desired properties of time–frequency energy distribution [5]. The Choi–William's distribution also known as exponential distribution (ED) [3] has a kernel $\phi(\theta,\tau) = \mathrm{e}^{-\theta^2\tau^2/\sigma}, \sigma > 0$. It retains the good properties of a TFR and provides a tradeoff between crossterm suppression and the frequency resolution through the parameter σ. Larger the value of σ, the ED is closer to WVD. That is, for large σ, ED has larger crossterms and good frequency resolution and vice versa. On the other hand, the cone-shaped kernel [20] only provides good time and frequency concentration and crossterms suppression. It does not attach much importance to the properties for the TFR. The reduced interference kernel [7] is an improved and generalized version of Choi–Williams distribution. In this direction, an application specific signal-dependent optimal kernel design [1], useful for different class of signals, is a major step. Based on orthogonal like Gabor expansion [14], a decomposition of the WVD achieves a balance between crossterms and useful properties. A denoising approach [4] based on shift-invariant wavelet packet decomposition has been proposed for adaptive suppression of crossterms.

To achieve a better frequency resolution for the WVD, the modified magnitude group delay (MMGD) for complex signals [11] has been used to remove the truncation effect or the ripple along the frequency axis, without using any *window function* [10]. For the instantaneous power spectrum, the MMGD for real signals [19] has been applied to overcome its undesired severe ringing effect, without compromising on frequency resolution [8]. The MMGD [19,11] basically removes the zeros close to the unit circle, without disturbing the poles of the signal. The spectral ripples and the associated white noise (with the signal) manifest as zeros close to the unit circle. Consequently, a reduction in the effect of *only these zeros*, results in a reduced ripple effect/variance of a spectral estimate, without any compromise on frequency resolution. However for the WVD, the residual crossterms left after time smoothing get enhanced due to the application of the MMGD and this requires a second time-smoothing [10].

Recently, a WVD based on signal decomposition approach, realized by a perfect reconstruction filter bank (PRFB), has been proposed [16]. The PRFB decomposes the multi-component signal into its components. The summation of their WVDs, results in a WVD whose crossterm and noise, are significantly reduced [16]. It is to be noted that in this approach also, the lag window used to overcome the truncation effect of the IACR, decides the frequency resolution and reduces it from that of a rectangular window.

In this paper, a new improved WVD (IWVD) has been proposed. The IWVD combines the signal decomposition by PRFB [16] for reducing the crossterms and the MMGD [10] for reducing the ripple effect due to truncation of the IACR [9]. The crossterm and the Gibb's ripple are reduced, without using any time and frequency smoothing. Therefore, the proposed WVD has a significantly superior performance over that of the PWVD, in terms of time and frequency resolution and in obeying the properties of a TFR. Further, its noise immunity is improved as the SD and the MMGD themselves individually offer an additional noise immunity.

2. The Wigner–Ville distribution [5]

For a signal $x(t)$, the WVD is defined as

$$W_x(t,\omega) = \int_{-\infty}^{\infty} x(t+\tau/2)x^*(t-\tau/2)\mathrm{e}^{-\mathrm{j}\omega\tau}\,\mathrm{d}\tau, \quad (1)$$

where $r(\tau) = [x(t+\tau/2)x^*(t-\tau/2)]$ is the *instantaneous autocorrelation* function and $*$ indicates conjugate operation. For computational purposes, it is necessary to weigh the signal by a window before evaluating the WVD and this window slides along the time axis with time instant t, where the WVD has to be evaluated. For a window function, $h(t)$, $h(t) = 0$ for $|t| > T/2$, the WVD of the windowed signal is

$$\mathrm{PW}_x(t,\omega) = \frac{1}{2\pi}\int_{-\infty}^{\infty} W_x(t,\xi)W_h(t,\omega-\xi)\,\mathrm{d}\xi, \quad (2)$$

where $W_h(t,\omega)$ is the WVD of the window function. This WVD of the windowed signal is called *Pseudo Wigner–Ville Distribution* (PWVD), $\mathrm{PW}_x(t,\omega)$. The effect of the window is to *smear* the WVD along the frequency axis. For a real symmetrical window,

$$\mathrm{PW}_x(t,\omega) = \int_{-\infty}^{\infty} [x(t+\tau/2)x^*(t-\tau/2)] \times h^2(\tau/2)\mathrm{e}^{-\mathrm{j}\omega\tau}\,\mathrm{d}\tau. \quad (3)$$

Effectively, the PWVD is the FT of the windowed function, $[x(t+\tau/2)x^*(t-\tau/2)]h^2(\tau/2)$. The window $h^2(\tau/2)$, generally not necessarily be factorizable and symmetric. The window *eats away* the correlation function at higher lags which results in a poor spectral resolution.

The quadratic operation on the signal, causes the WVD to be a bilinear transformation. For a composite signal with two components

$$x(t) = x_1(t) + x_2(t)$$

and for example, for $x_1(t) = \mathrm{e}^{\mathrm{j}(\omega_1 t+\phi_1)}$ and $x_2(t) = \mathrm{e}^{\mathrm{j}(\omega_2 t+\phi_2)}$,

$$W_x(t,\omega) = 2\pi\left[\delta(\omega-\omega_1)+\delta(\omega-\omega_2) + 2\delta\left(\omega-\frac{\omega_1+\omega_2}{2}\right)\cos\{(\omega_1-\omega_2)t + (\phi_1-\phi_2)\}\right].$$

The third term is the crossterm due to interference between the two components. The crossterm appears mid-way between two components of the signal. Its amplitude is proportional to product of the two components' amplitudes and it oscillates in time at a frequency equal to the frequency separation between them. The presence of the crossterm poses a major problem in the interpretation of the WVD of a multi-component signal. But as the crossterm oscillates in time, smoothing the WVD in time, attenuates the crossterm and enables a meaningful representation of the signal components, *but only at the cost of time resolution*.

The smoothing process, in time for crossterms and in frequency for the lag window, can be considered as a two-dimensional convolution of the WVD with a function $\Phi(t,\omega)$ [20,6] given by

$$\mathrm{SW}_x(t,\omega) = \frac{1}{2\pi}\int_{-\infty}^{\infty}\int_{-\infty}^{\infty} W_x(t,\omega) \times \Phi(t-\tau,\omega-\xi)\,\mathrm{d}\tau\,\mathrm{d}\xi, \quad (4)$$

where $\Phi(t,\omega) = \mathrm{FT}[\phi(\theta,\tau)]$, is a smoothing kernel. The kernel determines the properties of the distribution [6]. For WVD, $\phi(\theta,\tau)=1$. Using different smoothing kernels, a class of distribution known as *Cohen's class* [20,6] can be realized. Any smoothing will affect the properties of a time–frequency distribution (TFD) and the choice of this kernel depends upon the application. The properties of marginality in frequency, group delay and frequency support are not satisfied for common non-rectangular windows. This is due to smearing of the signal spectrum with that of the window. The time smoothing used in suppressing the crossterms does not permit the corresponding properties of a TFD in time. The objectives of the smoothing function $\phi(\theta,\tau)$ are to provide crossterm suppression, good time and frequency resolution and to have as many properties of a TFD as possible. As there is a tradeoff among these realizable objectives, the choice of this smoothing function has been a topic of research.

For the computation of an alias free Wigner distribution (WD) using FT, an analytic signal is required or the signal needs to be sampled at twice the Nyquist sampling rate. The aliasing effect occurs due to the very definition of WD. Its discrete version given below involves half-sample intervals $k/2$.

$$\mathrm{PW}_x(n,\omega) = \sum_k x(n+k/2)x^*(n-k/2)h^2(k/2)\mathrm{e}^{-\mathrm{j}\omega k} = 2\sum_p x(n+p)x^*(n-p)h^2(p)\mathrm{e}^{-2\mathrm{j}\omega p}.$$

For a signal sampled at Nyquist rate, the FT of the product $x(n+p)x^*(n-p)$ introduces aliasing as the sampling rate is reduced by a factor of 2 (i.e., $2p$ instead of p) and any particular frequency occurs at twice its value. Use of an analytic signal

$$x_a(n) = x(n) + \mathrm{j}\hat{x}(n) \quad \text{where } \hat{x}(n) \text{ is the Hilbert transform of } x(n)$$

overcomes the aliasing problem as the spectrum of $x_a(n)$ has nonzero values only for positive frequencies. In practice, the WD which uses an analytic signal as its input, is known as WVD. The use of an analytic signal necessitates further processing to be performed in complex domain.

3. Signal decomposition by perfect reconstruction filter bank [16]

The impulse response of the subfilters of a uniform filter bank are obtained by complex modulation of a lowpass filter and is given by

$$h_i(n) = h(n)e^{j\omega_i n}, \tag{5}$$

where

$$h(n) = \frac{1}{M}\frac{\sin(n\pi/M)}{n\pi/M} \quad \text{and} \quad \omega_i = 2\pi(i-1)/M, \quad i = 1,\ldots,M;$$

$h(n)$ is the impulse response of a prototype lowpass filter and M is the number of subfilters. Thus, the transfer function of the subfilters is

$$H_i(\omega) = H(\omega - \omega_i), \quad i = 1,\ldots,M.$$

The output from the ith subfilter is

$$z_i(n) = x(n) \otimes h_i(n),$$

$\otimes$: convolution.

For a perfect reconstruction, $h(n)$ should satisfy [16],

$$h(0) = 1/M,$$

$$h(mM) = 0, \quad \forall m \neq 0, \tag{6}$$

which, in the frequency domain, corresponds to

$$\sum_{i=1}^{M} |H(\omega - \omega_i)| = 1, \quad 0 \leqslant \omega \leqslant 2\pi. \tag{7}$$

The complex signal $z_i(n)$ becomes analytic, provided the Fourier transform of $z_i(n)$, $Z_i(\omega) = 0$ for $\omega < 0$. This will occur for all subfilters if $H(\omega) = 0$ for $|\omega| > \pi/M$. To achieve this, the real input $x(n)$ to the filter bank is band limited to the frequency interval $\{\pi/M, \pi - \pi/M\}$ [16]. Thus, the spectrum of $x(n)$ is covered by the subfilters indexed $i = 2,\ldots,M/2$, each having same bandwidth and form a uniform PRFB.

4. Modified magnitude group delay for a complex signal (MMGD) [19,11]

In this section, the GD for a complex signal and its modification [19] which reduces the variance without affecting the frequency resolution [11], will be reviewed.

4.1. GD for a complex signal [15]

If $x(n)$ is a minimum phase complex signal with its FT, $X(\omega)$,

$$\begin{aligned}\ln[X(\omega)] &= \sum_{n=0}^{\infty}[c(n)]e^{-j\omega n} \\ &= \sum_{n=0}^{\infty}[c_R(n) + jc_I(n)]e^{-j\omega n} \\ &= \sum_{n=0}^{\infty}[c_R(n)\cos\omega n + c_I(n)\sin\omega n] \\ &\quad + j\sum_{n=0}^{\infty}[-c_R(n)\sin\omega n + c_I(n)\cos\omega n].\end{aligned}$$

Also,

$$\ln[X(\omega)] = \ln[|X(\omega)|e^{j\theta(\omega)}] = \ln|X(\omega)| + j\theta(\omega).$$

Therefore,

$$\ln|X(\omega)| = \sum_{n=0}^{\infty}[c_R(n)\cos\omega n + c_I(n)\sin\omega n], \tag{8}$$

$$\theta(\omega) = \sum_{n=0}^{\infty}[-c_R(n)\sin\omega n + c_I(n)\cos\omega n], \tag{9}$$

$\theta(\omega)$ is the unwrapped phase and $c(n) = c_R(n) + jc_I(n)$ are cepstral coefficients. R and I refer to the real and imaginary parts. For a minimum phase signal, the log-magnitude spectrum and the phase are related by a single set of cepstral coefficients. The GD $\tau_m(\omega)$ is

given by

$$\tau_m(\omega) = \frac{-\partial\theta(\omega)}{\partial\omega} = \sum_{n=0}^{\infty} nc_{\mathrm{R}}(n)\cos\omega n + nc_{\mathrm{I}}(n)\sin\omega n = (1/2)\mathrm{FT}[nc(n) - nc*(-n)]. \tag{10}$$

If $nc(n)$ is conjugate symmetric, $\tau_m(\omega)$ is the FT of $nc(n)$ [15]. Since $c(n)$ sequence is derived from the magnitude, $\tau_m(\omega)$ is called as the magnitude GD for a complex signal (MGD).

4.2. Modification of the MGD [19,11]

In spectral estimation, the goal of achieving lower variance and high resolution is to capture a consistent spectral envelope and discard the fine structure, without affecting the former. One or a combination of the following three factors can result in fine structure/large variance of the signal spectrum estimate. They are (i) signal truncation effect, (ii) associated white noise, (iii) input white noise that drives a system in generating the signal. These factors introduce zeros close to the unit circle, which manifest as spikes in the GD and their effect cannot be removed by normal smoothing using a window function without any loss of frequency resolution. The periodogram spectral estimate, even at high noise levels, has a good frequency resolution, low bias and good ability to detect the signal, but its variance is large. For a given length of data, averaging the periodogram or windowed periodogram or smoothed GD, results in a reduced variance. But this will be at the expense of frequency resolution. The modification suggested in [19] removes the zeros close to the unit circle. Hence, the spikes in GD are removed effectively without disturbing the signal or system poles. The frequency resolution is therefore not sacrificed.

The modification basically considers the signal to be characterized by, a transfer function having only the denominator polynomial, generally known as an all-pole model. In such a case, the input driving noise to the transfer function or the associated noise with the signal or the truncation effect (zeros) on the signal corresponds to the numerator. The undesired effect of the numerator, viz., large variance is removed by dividing the transfer function by the numerator estimate without significantly disturbing the denominator. The GD domain provides a platform to do this operation, without any singularity problems, as it involves only multiplication and no division. The conventional variance reduction approach of averaging of the periodogram involves data segmentation and or windowing. This not only reduces the variance/effect of the numerator, but also the frequency resolution of the spectral peaks as it pulls signal poles towards the origin in addition to the zeros which are close to the unit circle.

Let $x(n)$ be a complex signal generated by an all-pole system driven by a white noise or it has sinusoids with white noise. Let its spectrum be represented by $X(\omega) = N(\omega)/D(\omega)$, $D(\omega)$ corresponds to the system or sinusoids and $N(\omega)$ to the excitation or the associated noise.

For this case, the MGD is

$$\tau_m(\omega) = \tau_{mN}(\omega) - \tau_{mD}(\omega), \tag{11a}$$

$\tau_{mN}(\omega)$ and $\tau_{mD}(\omega)$ are the MGDs for $N(\omega)$ and $D(\omega)$, respectively. Also, $\tau_m(\omega)$ is given by

$$\tau_m(\omega) = \frac{X_{m\mathrm{R}}(\omega)Y_{m\mathrm{R}}(\omega) + X_{m\mathrm{I}}(\omega)Y_{m\mathrm{I}}(\omega)}{|X(\omega)|^2}, \tag{11b}$$

where

$$X_m(\omega) = \mathrm{FT}[x_m(n)], \quad Y_m(\omega) = \mathrm{FT}[y_m(n)] \quad \text{and} \quad y_m(n) = nx_m(n),$$

$x_m(n)$ is the minimum phase equivalent of $x(n)$ and provides information only about the spectral magnitude. This is what is required for WVD at each instant of time and not the mixed phase information if any. Using Eqs. (8) and (9), $x_m(n)$ can be derived from the spectral magnitude $|X(\omega)|$.

Also [19],

$$\tau_m(\omega) = \frac{\alpha_N(\omega)}{|N(\omega)|^2} - \frac{\alpha_D(\omega)}{|D(\omega)|^2}. \tag{12}$$

From Eqs. (11a) and (12), $\alpha_N(\omega)$ and $\alpha_D(\omega)$ are the numerator of Eq. (11b) for $\tau_{mN}(\omega)$ and $\tau_{mD}(\omega)$, respectively.

The $\tau_{mN}(\omega)$ will have large amplitude spikes due to very small values of $|N(\omega)|^2$ near the zeros which are close to unit circle and this is not so with the $\tau_{mD}(\omega)$, as the roots of $D(\omega)$ are well within the unit circle. Hence, in $\tau_m(\omega)$, the effect of excitation or the associated noise or the signal truncation, masks the system or the signal component, which is assumed to be an all-pole one. By multiplying $\tau_m(\omega)$ by $|N(\omega)|^2$, the

effect of these zeros can be reduced. Also, as the envelope of $|N(\omega)|^2$ is nearly flat, the significant features of $\tau_{mD}(\omega)$ continue to exist, with the $|N(\omega)|^2$ fluctuations superimposed on it. Hence, the modified MGD (MMGD) $\tau_{\mathrm{mo}}(\omega)$, is

$$\tau_{\mathrm{mo}}(\omega) = \tau_m(\omega)|N(\omega)|^2. \tag{13}$$

The estimate of $|N(\omega)|^2$,

$$|\tilde{N}(\omega)|^2 = |X(\omega)|^2/|\bar{X}(\omega)|^2,$$

$|\bar{X}(\omega)|^2$ is the smoothed power spectrum obtained by the truncated cepstral sequence.

5. Improved Wigner–Ville distribution (IWVD)

In this proposed method [9,12], to avoid/reduce the occurrence of crossterms of the WVD, the multi-component signal is decomposed into its components using a uniform PRFB discussed in Section 3 with all filters having the same bandwidth. The individual IACRs of these components are added to get the complete IACR of the original signal [16]. Owing to the quadratic nature of IACR, the crossterms occur. The interaction of individual components is reduced as they are separated during the IACR computation. To remove the Gibbs ripple of the WVD without using any window function, the complete IACR that is significantly free from crossterms, will be subjected to MMGD.

The IACR of the original signal $r(n,k)$ at nth instant and for lag k is

$$r(n,k) = \sum_{i=2}^{M/2} r_i(n,k), \tag{14}$$

$r_i(n,k)$ is the IACR of the ith component of the signal.

In the PRFB, if the signal is confined to the frequency interval $\{\pi/M, \pi-\pi/M\}$, the filter bank generates directly the required analytic signal for the WVD and hence avoids the computation of the Hilbert transform of the signal. Since the filterbank is a perfect reconstruction one, the signal decomposition prior to computation of the WVD kernel does not introduce any errors in the performance of the WVD.

To remove the Gibbs ripple of the WVD, the IACR $r(n,k)$ that is significantly free from crossterms, will be subjected to MMGD for a complex signal, since the IACR of a WVD is complex.

In the MMGD described in Section 3, the numerator estimate is

$$\tilde{N}(\omega) = \frac{X(\omega)}{\bar{X}(\omega)} = \left[1 + \frac{\Delta(\omega)}{\bar{X}(\omega)}\right]. \tag{15a}$$

Here, $\Delta(\omega)$ represents the fluctuating part of $X(\omega)$. For a signal having a *flat spectral envelope* characteristic, in the GD $\tau_m(\omega)$, the contribution is only due to $\Delta(\omega)$. A $\tau_{\mathrm{mo}}(\omega)$, free from fluctuations, is given by [10,8]

$$\tau_{m\Delta}(\omega) = \tau_m(\omega)|\Delta(\omega)|^2. \tag{15b}$$

Presently for the WVD, it is required to remove the ripple on the floor. This is equivalent to ripples on a flat spectral envelope characteristic. The MGD $\tau_m(\omega)$ has to be derived from the Fourier transform (FT) of the crossterm free IACR using Eqs. (8) and (10). The FT of IACR represents the instantaneous power density spectrum (PSD) and at each frequency bin, it is supposed to be a positive quantity. This may not be so as the PSD gets convolved with the bipolar valued *sinc function*, the FT of the inevitably present rectangular window. Since computation of $\tau_m(\omega)$ involves logarithmic operation, it is necessary to ensure that FT of IACR is positive. This is achieved by raising the floor level sufficiently by scaling up the IACR at the zeroth lag [18, pp. 59–60]. The equivalent magnitude spectrum is obtained from positivity ensured PSD. Further, the linearly weighted cepstral coefficient sequence is made conjugate symmetric [10].

For the proposed improved WVD (IWVD), at each time instant, a spectrum that is significantly free from the crossterm and Gibbs ripple effect is obtained. This also has a better frequency and time resolution. The spectrum is obtained from $\tau_{\mathrm{mo}}(\omega)$ using Eq. (15b) by retracing the MGD computation procedure in the reverse order. Here, the cepstral coefficient sequence derived from $\tau_{\mathrm{mo}}(\omega)$ has to be made conjugate symmetric. For each TFR slice obtained by the MMGD, subtraction of the mean value and addition of the scaled mean value, restore the original floor level.

The proposed IWVD preserves the frequency resolution of a rectangular window as there is no smoothing along the frequency axis due to absence of any

window function in removing the Gibb's ripple. As the crossterms are not significantly allowed to exist by signal decomposition, there is no time smoothing. Hence, the IWVD can be expected to provide a better time resolution than that of a time smoothed WVD. The desired properties of a TFR namely, the marginals, instantaneous parameters and support properties are expected to be obeyed relatively better by the IWVD than by the PWVD.

In the IWVD as there is no time smoothing, its time resolution is better than that of WVD that uses only MMGD for the ripple reduction. Further, in IWVD as the crossterms are *not significantly allowed to exist*, there is no enhancement of residual crossterms by MMGD. Therefore, *IWVD does not require a second smoothing in time*. Also, its frequency resolution is better than that of the WVD that uses only signal decomposition.

The signal decomposition not only reduces interaction between signal components but also for the noisy components, it significantly avoids crossterms due to noise and hence has a better noise immunity. As MMGD not only removes the zeros due to ripple effect but also those due to noise, it provides additional noise immunity. Hence, the IWVD based on signal decomposition and MMGD, provides improved noise immunity.

Thus, the novelty of the algorithm is that it is able to reduce the Gibbs ripple without using any window function and reducing the crossterms significantly without time smoothing as they are not significantly allowed to exist by signal decomposition. As no window is used it preserves the frequency resolution of a rectangular window and absence of time smoothing improves time resolution. These further enable the proposed method to obey the desired properties of TFR to a better extent.

5.1. Algorithm for IWVD

Step 1: Decompose the signal into its components using the perfect reconstruction filter bank.

For this:

(i) Design a filter bank with M subfilters with impulse responses given by Eq. (5). The length of $h(n)$ is chosen to get a desired transition width and $h(n)$ is weighted by a Kaiser window with a suitable smoothing parameter to obtain a desired stopband attenuation.

(ii) For a real input signal $x(n)$ with its spectrum in the region $(\pi/M, \pi-\pi/M)$, (π corresponds to half the sampling frequency) obtain its components which are analytic by computing the outputs for filters indexed from $i = 2, \ldots, M/2$.

Step 2: Compute the IACR $r(n,k)$.

For this:

(i) Compute IACR for the ith signal component, $r_i(n,k)$, for each value of lag k ($k = 0, 1, \ldots, K$),

$$r_i(n,k) = \{x_i(n-k)x_i^*(n+k)\} \quad \text{for } -T \leqslant n \leqslant T.$$

(ii) Compute $\bar{r}(n,k)$, the IACR of the original signal at nth instant and for lag k by

$$\bar{r}(n,k) = \sum_{i=2}^{M/2} r_i(n,k).$$

(iii) $r(n,k)$, the IACR for the *complete range* of k ($-K, \ldots, -1, 0, 1, \ldots, K$), rearranged for the discrete Fourier transform (DFT) array (of length N) is given by

$$r(n,k) = \begin{cases} \bar{r}(n,k), & k = 0, 1, \ldots, K, \\ 0, & k = K+1, \ldots, \\ & Q-K-1, \\ \bar{r}^*(n, Q-k), & k = Q-k, \ldots, Q-1. \end{cases}$$

Step 3: At a particular instant $n = n_1$, compute the MGD $\tau_m(l)$ (Eqs. (8) and (10)), l is the discrete frequency bin index.

For this:

(i) Compute the *definitely positive* power spectral density $\mathrm{IP}(n_1, l)$ by

$$\mathrm{IP}(n_1, l) = \mathrm{Re}[\mathrm{DFT}\{r_p(n_1,k)\}],$$

$$r_p(n_1,k) = \begin{cases} Ur(n_1,0), & k = 0,\ U \gg 1, \\ r(n_1,k), & k \neq 0. \end{cases}$$

(The factor U enhances the value of the autocorrelation at zeroth lag and in turn lifts the floor level. Hence, the positivity of the PSD is ensured by the proper choice of the factor U.)

(ii) Compute the cepstrum $\{c(k)\}$:

$$\mathrm{IM}(n_1,l)=0.5\ln[\mathrm{IP}(n_1,l)],$$

$$\{c(k)\}=\mathrm{IDFT}[\mathrm{IM}(n_1,l)],$$

where IDFT is the inverse DFT.

(iii) Compute the MGD $\tau_m(l)$: For this generate the sequence $\{g(k)\}$

$$g(0)=(0,0),$$

$$g_{\mathrm{R}}(k)=kc_{\mathrm{R}}(k),\quad g_{\mathrm{I}}(k)=kc_{\mathrm{I}}(k),$$

$$k=1,\ldots,Q/2,$$

$$g_{\mathrm{I}}(k)=0,\quad k=Q/2,$$

$$g(k)=g_{\mathrm{R}}(k)+g_{\mathrm{I}}(k),\quad k=1,\ldots,Q/2,$$

$$g(Q-k)=g^*(k),\quad K=1,\ldots,Q/2,$$

then

$$\tau_m(l)=\mathrm{Re}[\mathrm{DFT}\{g(k)\}].$$

Step 4: Compute the modified GD, GDM $\tau_{m\Delta}(l)$ (Eqs. (15a) and (15b)).

For this:

(i) Compute the estimate $\Delta(l)$:

(a) Estimate the smoothed log spectrum $\bar{\mathrm{IM}}(n_1,l)$:

$$f(k)=\begin{cases}c(k), & k=0,1,\ldots,P,\\ c(k), & k=Q-P,\ldots,Q-1,\\ 0, & k=P+1,\ldots,Q-P+1,\end{cases}$$

P is the cepstrum truncation length,

$$\bar{\mathrm{IM}}(n_1,l)=\mathrm{Re}[\mathrm{DFT}[f(k)]].$$

(b) Estimate, $\Delta(l)$ using:

$$\hat{N}_e(l)=\mathrm{IM}(n_1,l)-\bar{\mathrm{IM}}(n_1,l),$$

$$\hat{N}(l)=\exp[\hat{N}_e(l)],$$

and

$$\Delta(l)=(\hat{N}(l)-1)\exp\{\bar{\mathrm{IM}}(n_1,l)\}.$$

(ii) Compute $\tau_{m\Delta}(l)$ by $\tau_{m\Delta}(l)=\tau_m(l)|\Delta(l)|^2$.

Step 5: Compute the improved TFR slice at time n_1. For this:

(i) Compute the sequence $s(k)$ from $\tau_{m\Delta}(l)$ (using Eq. (3c)): For this

$s_1(k)=\mathrm{IDFT}[\tau_{m\Delta}(l)]$, and $\{s(k)\}$ is given by

$$s(0)=(0,0),$$

$$s_{\mathrm{R}}(k)=s_{1\mathrm{R}}(k)/k,\quad s_{\mathrm{I}}(k)=s_{1\mathrm{I}}(k)/k,$$

$$k=1,\ldots,Q/2,$$

$$s_{\mathrm{I}}(k)=0,\quad k=Q/2,$$

$$s(k)=s_{\mathrm{R}}(k)+s_{\mathrm{I}}(k),\quad k=1,\ldots,Q/2,$$

$$s(Q-k)=s^*(k),\quad K=1,\ldots,Q/2.$$

(ii) Compute estimate $S(l)$: $S(l)=\mathrm{Re}[\mathrm{DFT}\{s(k)\}]$.

(iii) Obtain the normalized estimate $S_N(l)$ by scaling $S(l)$ with respect to $\mathrm{IM}(n_1,l)$:

$$A_1=\frac{1}{Q}\sum_{l=0}^{Q-1}S(l),\quad S_m(l)=S_m(l)-A_1,$$

$$A_2=\frac{1}{Q}\sum_{l=0}^{Q-1}\mathrm{IM}(n_1,l),$$

$$\mathrm{IM}_m(n_1,l)=\mathrm{IM}(n_1,l)-A_2,$$

$$G=\max[S_m(l)]/\max[\mathrm{IM}_m(n_1,l)],$$

$$S_N(l)=\frac{S_m(l)}{G}+A_2.$$

(iv) The improved WVD slice estimate $\mathrm{IWVD}(n_1,l)$ is obtained from $S_N(l)$:

$$S1(l)=\exp[2S_N(l)],\quad B=\frac{1}{M}\sum_{l=0}^{M-1}S1(l),$$

$$\mathrm{IWVD}(n_1,l)=S1(l)-B+\frac{B}{U}.$$

Step 6: Repeat steps 3–5 for each sample instant n, in the time interval considered and obtain the $\mathrm{IWVD}(n,l)$.

Steps 1–6 form the algorithm for IWVD.

A direct implementation of the new algorithm certainly requires more computations than the PWVD. But for an efficient implementation, some of the fast approaches available in the literature can be directly

made use off or the algorithm can be reformulated for this purpose. As mentioned already, this algorithm does not involve Hilbert transformation (HIT) in generating the analytic signal, weighing of the IACR by a window function and time smoothing of the IACR for each lag. However, since $r_i(n,k)$ has to be computed for $i=2,\ldots,M/2$, the number of computations is $(M/2-1)$ times that of a single IACR used in PWVD. The computations involved in each $r_i(n,k)$ can be reduced by a factor M by resorting to decimation and interpolation provided the computational load of these operations is less than that of direct computation of $r_i(n,k)$. Further, the PRFB can be implemented efficiently using a polyphase FFT approach [18].

The Hartley transform is known for its computational and memory efficiency as it saves both by about 50% [17]. This is due to the fact that unlike FT, it *involves only real and no complex arithmetic operations* and efficient fast algorithms have been developed for Hartley transform (FHT) [2]. This has been advantageously used both for computing the WVD [13] and cepstrum [17]. The Hartley transform of $x(n)$ is

$$\mathrm{HART}[x(n)] = \sum_{-M}^{M} x(n)[\cos\omega n + \sin\omega n].$$

A complex conjugate symmetric signal $x(n)$ can be expressed as $x(n) = x_e(n) + jx_o(n)$, $x_e(n)$ and $x_o(n)$ are even and odd part of $x(n)$. Then,

$$\begin{aligned} X(\omega) &= \sum_{-M}^{M} x(n)e^{-j\omega n} \\ &= \sum_{-M}^{M} (x_e(n) + jx_o(n))e^{-j\omega n} \\ &= \sum_{-M}^{M} x_e(n)\cos\omega n + x_o(n)\sin\omega n \\ &= \sum_{-M}^{M} (x_e(n) + jx_o(n))(\cos\omega n + \sin\omega n), \\ X(\omega) &= \mathrm{HART}[x_e(n) + jx_o(n)]. \end{aligned}$$

Since the Hartley transform involves only real operations it will bring down the computational load and the memory requirement by 50%. *As IACR and the cepstrum involved for the WVD are conjugate symmetric, the FHT is directly applicable.*

The WVD requires 3 FHTs (two for the HIT and one to take the FT of the IACR) compared to 3 complex FFTs. To compute the proposed IWVD TFR slice, totally 6 FHTs (3 for the step 3 and 1 for step 4 and 2 for step 5) are required. There is no windowing and time smoothing. These points will be helpful in developing an efficient algorithm for the proposed IWVD.

6. Simulation results

The performance of the proposed IWVD is illustrated both for FSK and chirp signals. The performance of this method is compared with three existing methods namely:

(1) WVD with lag window and time smoothing (PWVD),
(2) WVD with signal decomposition and lag window (FBWVD) and
(3) WVD with MMGD and time smoothing (GDWVD).

In all the examples, the number of lags considered is 31. Further, discrete Fourier transform of length 128, is used, in all the cases.

For signal decomposition, a PRFB with six subfilters is used. Prototype low pass filter is designed by window method. All the other filters of the uniform PRFB are got by complex modulation of the prototype filter. Kaiser window with a smoothing factor of 8 is employed to reduce stop band and pass band ripple in the frequency response. Impulse response length of each filter is 128. *Marginally overlapping filters* (*also known as nonoverlapping filters*) are used (Fig. 1a).

In the methods where filterbank is not employed, the analytic signal is derived using the Hilbert transform of the original real signal. The Hilbert transform has been realized in time domain by convolving the signal with the impulse response of the Hilbert transformer. However, in the methods where filterbank is employed, to compute the IACR of filter outputs, the analytic signals are derived by considering filters indexed from 2 to $M/2$. For six subfilters, the analytic signals are obtained from second and third filters.

TFR slices, by GDWVD and PWVDs for an FSK signal for the same instant of time, are shown in Fig. 1b, c and d. GDWVD and PWVDs use

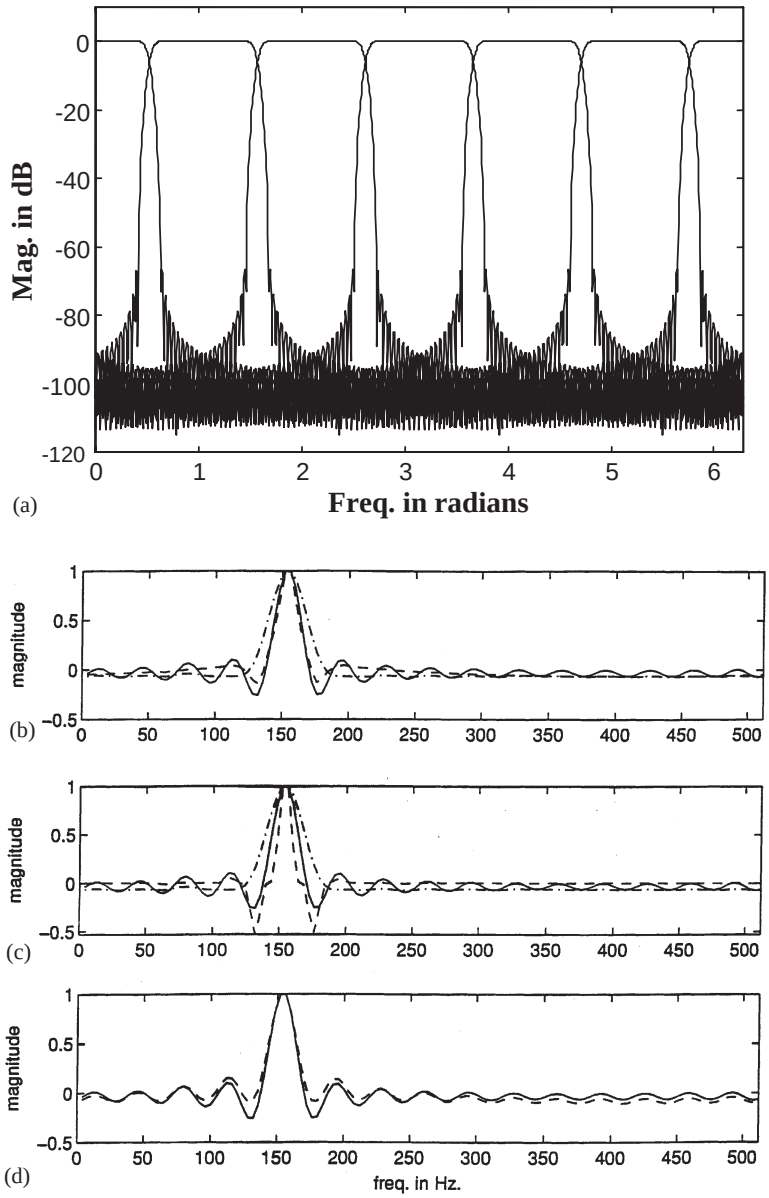

Fig. 1. (a) Frequency response of filters. (b–d) Comparison of the resolution and ripple reduction by PWVDs using RW and HW and GDWVD. WVD slice by (b): —— PWVD by RW, – · – · – PWVD by HW, - - - - GDWVD; (c): —— PWVD by RW, – · – · – PWVD by HW, - - - - MMGD; (d): —— PWVD by RW, - - - - GDWD by $|\hat{N}(\omega)|^2$.

rectangular window (RW) and Hamming window (HW). This clearly brings out the effect of the MMGD in reducing the Gibbs ripple. The GDWVD not only reduces the ripple significantly, but also preserves the frequency resolution provided by that of the RW (Fig. 1b). The PWVD that uses RW has a better frequency resolution than the one that uses HW, but suffers from Gibbs ripple. On the other hand, the PWVD that uses HW reduces the Gibbs ripple at the cost of frequency resolution.

This is because the effective lag length of the IACR is reduced due to the application of HW. Fig. 1c shows that the MMGD provides an additional frequency resolution over that of the RW. This is due to the very nature of GD. Fig. 1d shows that to suppress the Gibbs ripple while preserving the frequency resolution of an RW, $\tau_m(\omega)$ has to be multiplied by $|\Delta(\omega)|^2$ and not by $|\hat{N}(\omega)^2|$. This is due to the fact that the fluctuations in the latter are different from those required to be cancelled in $\tau_m(\omega)$.

For FSK signal, the TFR and their corresponding contour plots are shown in Fig. 2a–d and Fig. 2e–f, respectively. In PWVD, a 5-point boxcar smoothing is applied to IACR for each lag, along the time axis and this reduces the crossterms (Fig. 2a and e). By decomposing the signal into its components with the PRFB, and then summing the individual IACRs, the FBWVD gives a TFR *almost free* from crossterms. This can be clearly seen by comparing Fig. 2b and f with Fig. 2a and e. It is to be noticed that even the residual crossterm magnitude of the PWVD is comparatively appreciable. The FBWVD preserves the time resolution of WVD, as no time smoothing is applied. However, since in PWVD and FBWVD, IACRs are weighted by an HW to reduce the Gibbs ripple, the frequency resolution is poorer than that of WVD.

In GDWVD and IWVD, MMGD is applied to IACRs of PWVD and FBWVD, respectively. To avoid the negative spectral values in the PSD, the IACRs of PWVD and FBWVD at zeroth lag have been lifted by a factor of 100. As seen from the figures (Fig. 2c and g) and (Fig. 2d and h), application of MMGD not only preserves the frequency resolution of WVD but also removes Gibbs' ripples. This is also evident from Fig. 1b. However, in GDWVD the *residual crossterms left after time smoothing also gets enhanced* (Fig. 2c and g). This enhanced crossterm effect can be significantly reduced by a second smoothing in time [10] (not shown in figure). With the IWVD, the second smoothing is not required as the crossterms are *almost not allowed* to exist due to signal decomposition prior to computing the IACR. With PWVD, even its residual crossterms have appreciable magnitude. Therefore, the IWVD crossterm suppression is quite significant compared to that of the PWVD. Hence in IWVD, preserving the time and frequency resolutions of the WVD, the crossterms are almost not allowed to exist and the Gibbs ripple is significantly reduced (Fig. 2d and h). In both the cases, the $|\Delta(\omega)|^2$ estimate is obtained by considering the initial 6-cepstral coefficients in computing the smoothed PSD.

These results indicate that the proposed IWVD is very effective in removing the crossterms and Gibbs ripple while preserving the time and frequency resolutions of the WVD, compared to that of the PWVD or GDWVD or FBWVD.

For the crossing linear chirp signal, the TFRs and their respective contour plots are shown in Fig. 3a–d and in Fig. 3e–f, respectively. Results similar to those in FSK signal are observed for PWVD (Fig. 3a and e) and FBWVD (Fig. 3b and f). To reduce crossterms, a 5-point boxcar smoothing along time axis is applied to IACR. Further, for both PWVD and FBWVD, to ensure positivity of the PSD, the IACR at the zeroth lag is increased by a factor of 400. For the estimation of $|\Delta(\omega)|^2$, the first 8-cepstral coefficients are used in computing the smoothed PSD. In GDWVD (Fig. 3c and g) ridge type of effect occurs at the region of crossing of the two chirps. This can be reduced by a second smoothing, along the time axis [10] (not shown figure). As in the case of FSK signal, the IWVD (Fig. 3d and h) reduces the crossterms and Gibbs ripple preserving both frequency and time resolutions.

For the above signals in the presence of noise having a signal-to-noise ratio (SNR) of 3 dB, the performance of PWVD, FBWVD, GDWVD and IWVD, are shown in Figs. 4 and 5, respectively. For FSK and chirp signals, cepstral sequences having the initial 6 and initial 16 coefficients, respectively, are used in the estimation of $|\Delta(\omega)|^2$. The IWVD is very effective in removing the spurious spectral peaks due to noise while preserving the frequency resolution, compared to other methods, considered. This is to be expected. The WVDs independently obtained by using the modified group delay and by signal decomposition, by themselves, have an additional immunity to noise compared to the PWVD.

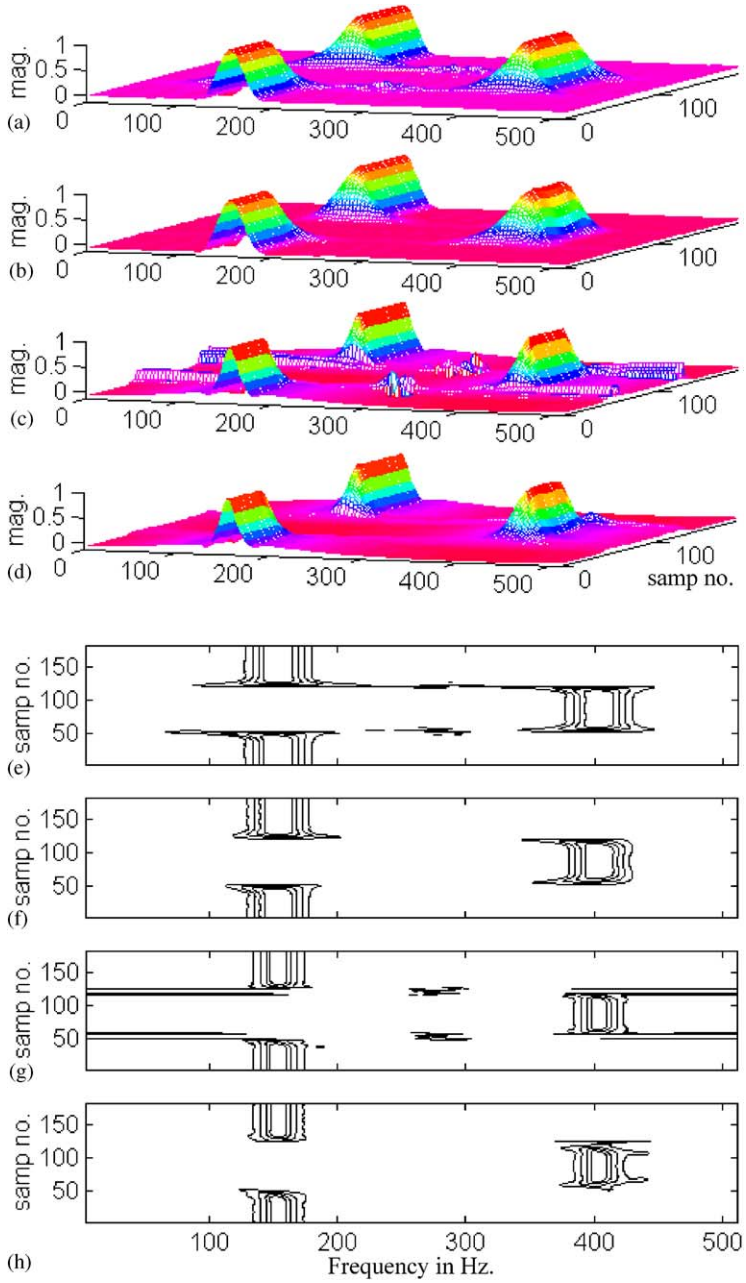

Fig. 2. TFR of FSK signal by (a) PWVD, (b) FBWVD, (c) GDWVD and (d) IWVD. (e)–(h) Contour plots of (a), (b), (c) and (d), respectively.

Thus, for FSK and crossing linear chirp signals, the above results indicate that there is a significant improvement in the performance of the proposed IWVD, in terms of crossterms suppression, Gibbs ripple reduction and noise immunity over those of PWVD, FBWVD and GDWVD.

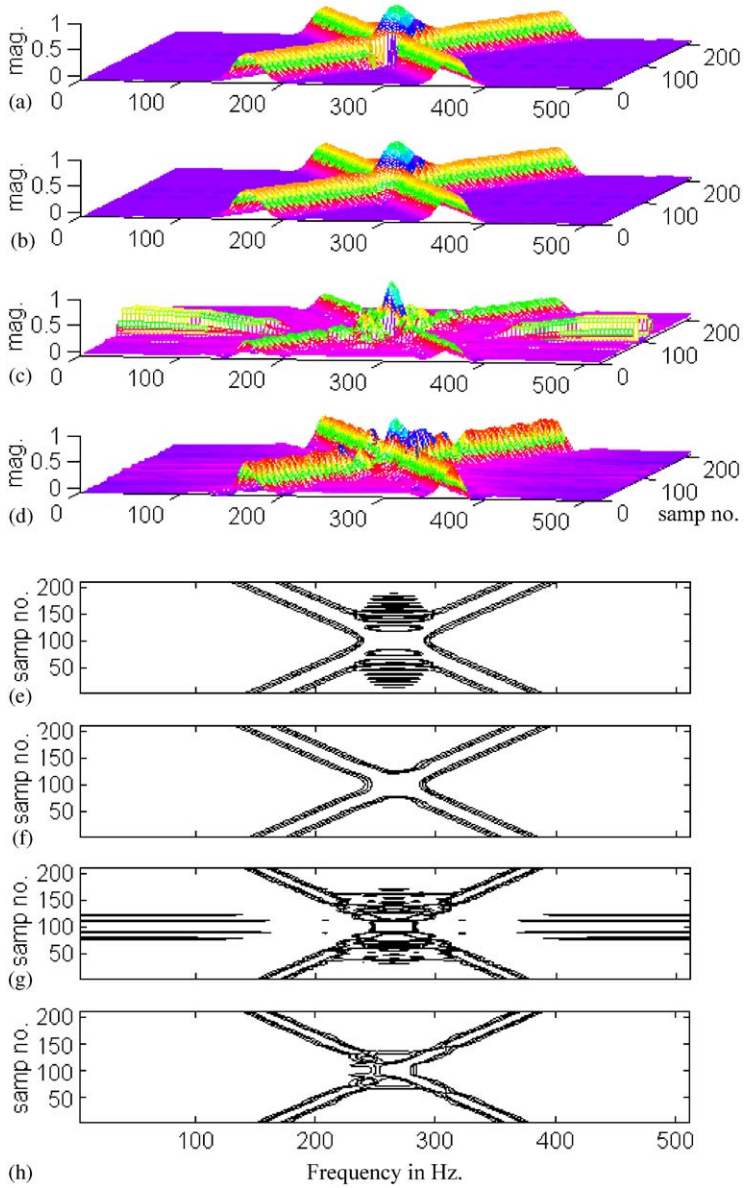

Fig. 3. TFR of chirp signal by (a) PWVD, (b) FBWVD, (c) GDWVD and (d) IWVD. (e)–(h) Contour plots of (a), (b), (c) and (d), respectively.

The crossterms suppression and Gibbs ripple reduction are achieved without much compromise on frequency and time resolution. Further, as there is no frequency and time smoothing, the IWVD is expected to obey better, the desired properties of a TFR compared to the WVDs, which use either time or frequency smoothing or both.

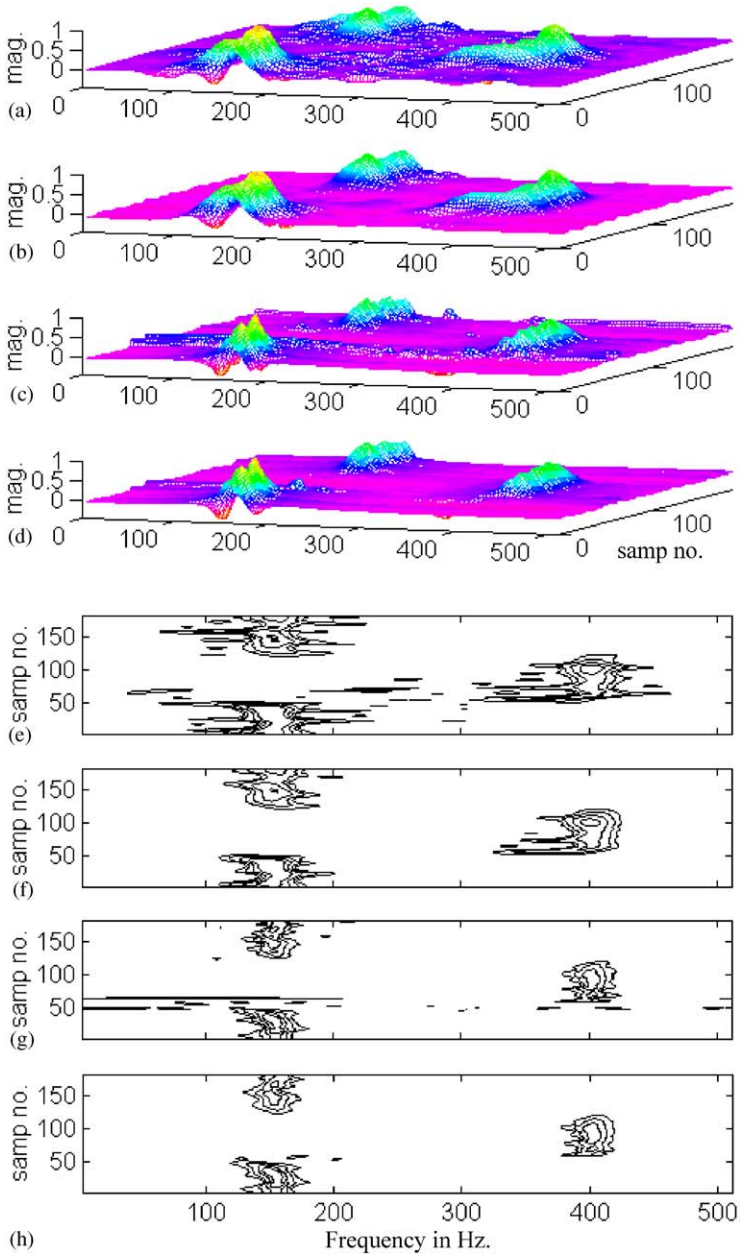

Fig. 4. TFR of FSK signal with white noise by (a) PWVD, (b) FBWVD, (c) GDWVD and (d) IWVD. (e)–(h) Contour plots of (a), (b), (c) and (d), respectively.

7. Conclusions

In this paper, a new improved WVD was proposed that combines the signal decomposition by PRFB for reducing the existence of crossterms, and the MMGD for reducing the Gibbs ripple effect due to truncation of the IACR. The crossterms and the Gibbs ripple are significantly reduced, without using any time

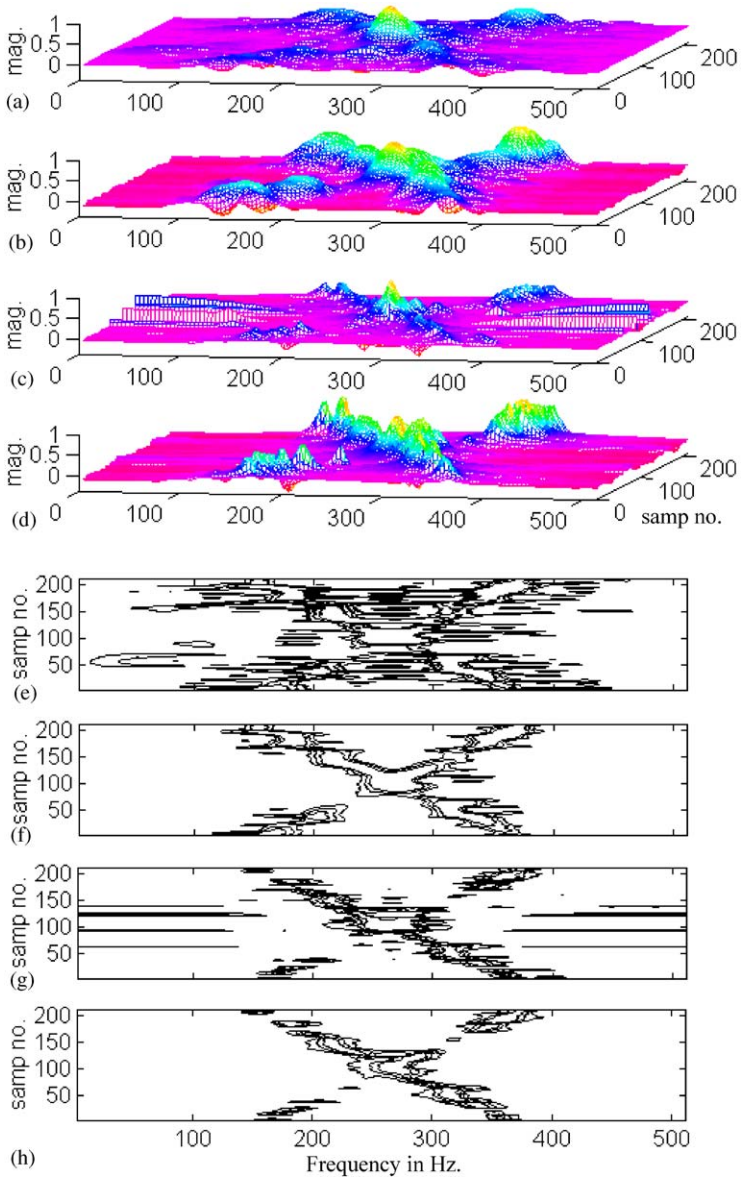

Fig. 5. TFR of chirp signal with white noise by (a) PWVD, (b) FBWVD, (c) GDWVD and (d) IWVD. (e)–(h) Contour plots of (a), (b), (c) and (d), respectively.

smoothing and common window function for the IACR, respectively. Therefore, the performance of the proposed WVD is significantly superior to those of the PWVD and its considered versions, in (i) time and frequency resolution, (ii) noise immunity and (iii) obeying properties of a TFR.

From the implementation point of view, the computational complexity of different algorithms, is of importance. This complexity reduction can be the subject of future study. This investigation aimed at the exploitation of signal decomposition and modified group delay for the reduction of crossterm and Gibbs

ripple without compromise on time and frequency resolutions. The proposed object has been realized and demonstrated.

Acknowledgements

The Authors thank Mrs. Padma Madhuranath and Dr. G. Girija, Flight Mechanics and Control Division, N.A.L. Bangalore; for correcting manuscript from the point of view of English language.

References

[1] R.G. Baraniuk, D.L. Jones, A signal dependent time–frequency representation optimal kernel design, IEEE Trans. Signal Process. 41 (4) (April 1993) 1589–1601.
[2] R.N. Bracewell, The fast Hartley transform, Proc. IEEE 72 (1986) 1010–1018.
[3] H.I. Choi, W.J. Williams, Improved time frequency representation of multicomponent of signals using exponential kernels, IEEE Trans. Signal Process. 37 (6) (1989) 862–871.
[4] I. Cohen, S. Raz, D. Malah, Adaptive suppression of Wigner interference terms using shift-invariant wavelet packet decompositions, Signal Processing 73 (1999) 203–223.
[5] L. Cohen, Time–frequency distribution—a review, Proc. IEEE 77 (1989) 941–981.
[6] P. Flandrin, Some features of time–frequency representation of multicomponent signals, International Conference on Acoustics, Speech and Signal Processing, 1984, pp. 41B4.1–41B.4.4.
[7] J. Jeong, W.J. Williams, Kernel design for reduced interference distributions, IEEE Trans. Signal Process. 40 (2) (1992) 402–412.
[8] S.V. Narasimhan, Improved instantaneous power spectrum (IPS) performance: a group delay approach, Signal Processing 80 (2000) 75–88.
[9] S.V. Narasimhan, M.B. Nayak, Improved Wigner–Ville distribution performance by signal decomposition and modified group delay, Proceedings of International Conference on Communication, Control and Signal Processing (CCSP-2000), Bangalore, India, July 26–28, 2000, pp. 35–39.
[10] S.V. Narasimhan, E.I. Plotkin, M.N.S. Swamy, Power spectrum estimation of complex signals and its application to Wigner–Ville distribution: a group delay approach, Sadhana 23 (Part-1) (1998) 57–71.
[11] S.V. Narasimhan, E.I. Plotkin, M.N.S. Swamy, Power spectrum estimation of complex signals: group delay approach, Electron. Lett. 35 (25) (December 1999) 2182–2184.
[12] M.B. Nayak, Improved Wigner–Ville distribution by signal decomposition, modified group delay and modeling, M.Tech. Thesis, Department of Electronics & Communication Engineering, Karnataka Regional Engineering College, Surathkal 574157, Karnataka, India, July 2000.
[13] S.C. Pei, I.I. Yang, Computing pseudo Wigner distribution by the fast Hartley transform, IEEE Trans. Signal Process. 40 (9) (1992) 2346–2349.
[14] S. Quian, D. Chen, Decomposition of the Wigner–Ville distribution and time frequency distribution series, IEEE Trans. Signal Process. 42 (10) (1994) 2836–2842.
[15] G.R. Reddy, V.V. Rao, Group delay functions for complex signals, Signal Processing 12 (1987) 5–15.
[16] F. Sattar, G. Salomonsson, The use of a filter bank and the Wigner–Ville distribution for time–frequency representation, IEEE Trans. Signal Process. 47 (1999) 1776–1783.
[17] M.C. Steckner, D.J. Drost, Fast cepstrum analysis using the Hartley transform, IEEE Trans. Acoust. Speech Signal Process. 37 (8) (1989) 1300–1302.
[18] P.P. Vaidyanathan, Mutirate Systems and Filter Banks, Prentice-Hall, Englewood Cliffs, NJ, 1993, pp. 59–60.
[19] B. Yegnanarayana, H.A. Murthy, Significance of group delay functions in spectral estimation, IEEE Trans. Signal Process. 40 (9) (1992) 2281–2289.
[20] Y. Zhao, L. Atlas, R. Marks II, The use of cone shaped kernels for generalized time–frequency representation of nonstationary signals, IEEE Trans. Signal Process. 38 (7) (1990) 1084–1091.